Supporting Information for

Partitioning the Uncertainty of Ensemble Projections of Global Glacier Mass Change

Ben Marzeion, Regine Hock, Brian Anderson, Andrew Bliss, Nicolas Champollion, Koji Fujita, Matthias Huss, Walter Immerzeel, Philip Kraaijenbrink, Jan-Hendrik Malles, Fabien Maussion, Valentina Radić, David R. Rounce, Akiko Sakai, Sarah Shannon, Roderik van de Wal, and Harry Zekollari

Contents of this file

Overview over supplementary figures

Figure	Variable	Scenario
S1	specific mass balance	RCP2.6
S2		RCP4.5
S3		RCP6.0
S4		RCP8.5
S5	glacier area change relative to 2015	RCP2.6
S6		RCP4.5
S7		RCP6.0
S8		RCP8.5
S9	rates of glacier mass loss	RCP2.6
S10		RCP4.5
S11		RCP6.0
S12		RCP8.5
S13	temporally accumulated glacier mass loss since 2015	RCP2.6
S14		RCP4.5
S15		RCP6.0
S16		RCP8.5
S17	glacier mass relative to 2015	RCP2.6
S18		RCP4.5
S19		RCP6.0
S20		RCP8.5
S21	absolute contribution of each source of uncertainty to the total uncertainty of projected mass loss rates	n/a
S22	relative contribution of each source of uncertainty to the total uncertainty of projected mass loss rates	n/a
S23	absolute contribution of each source of uncertainty to the total uncertainty of projected mass loss accumulated since 2015	n/a

Overview over supplementary tables

Table	Description
S1	definition of years in each glacier model's submitted annual volume and area time-series
S2	summary of bias correction, downscaling, and calibration and evaluation of modeled mass balance for each glacier model

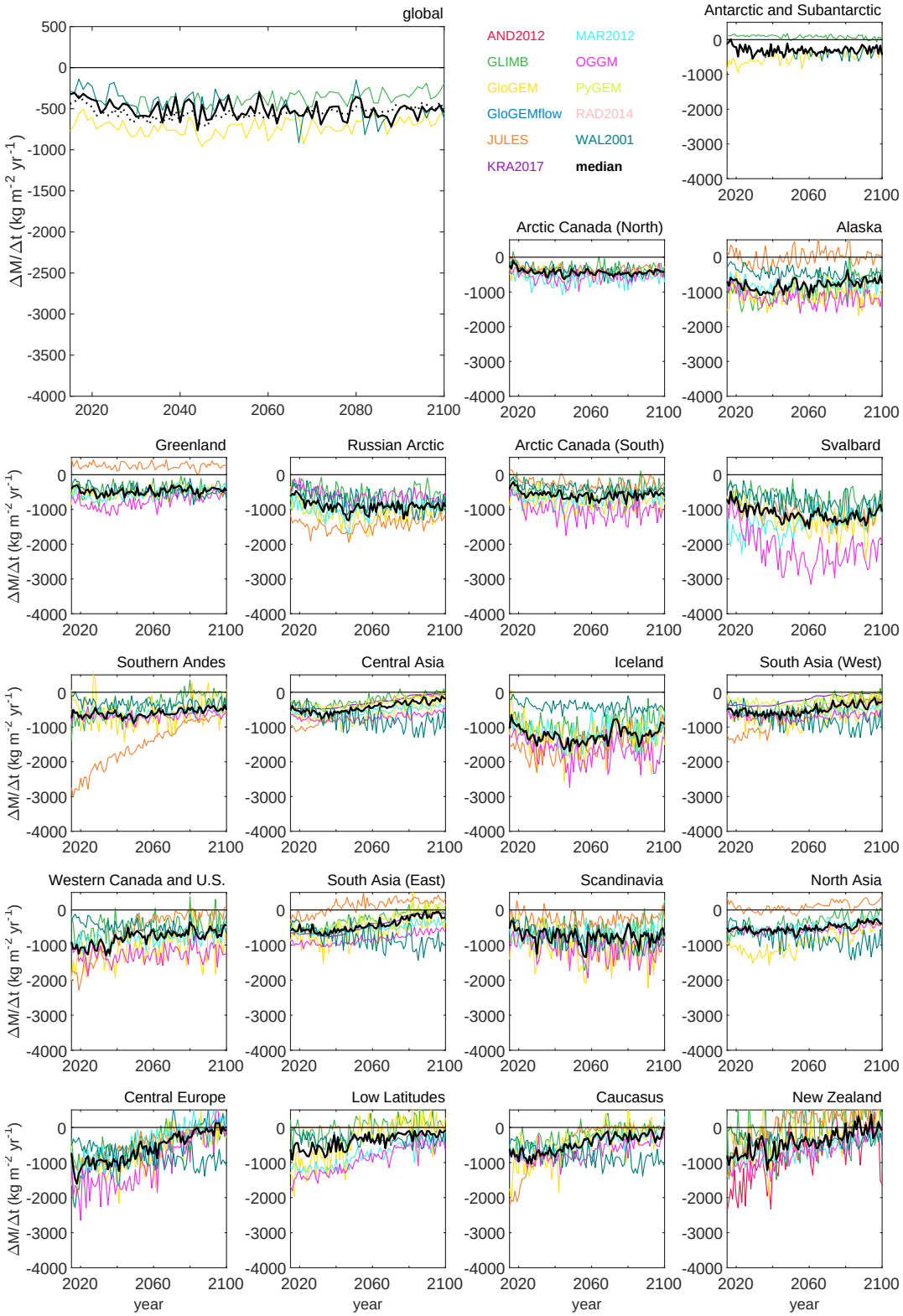

Figure S1 Specific mass balance in kg m^{-2} yr^{-1} as a function of time and glacier model, for scenario RCP2.6. Colored solid lines indicate the medians of each glacier model's multi-GCM projections. Global panel: dotted black line indicates average of all regional ensemble medians, weighted by glacier area of the respective region. Solid black line indicates median of the medians of each glacier model's multi-GCM projections with global coverage. Regional panels: black lines indicate median of the medians of each glacier model's multi-GCM projections covering that region.

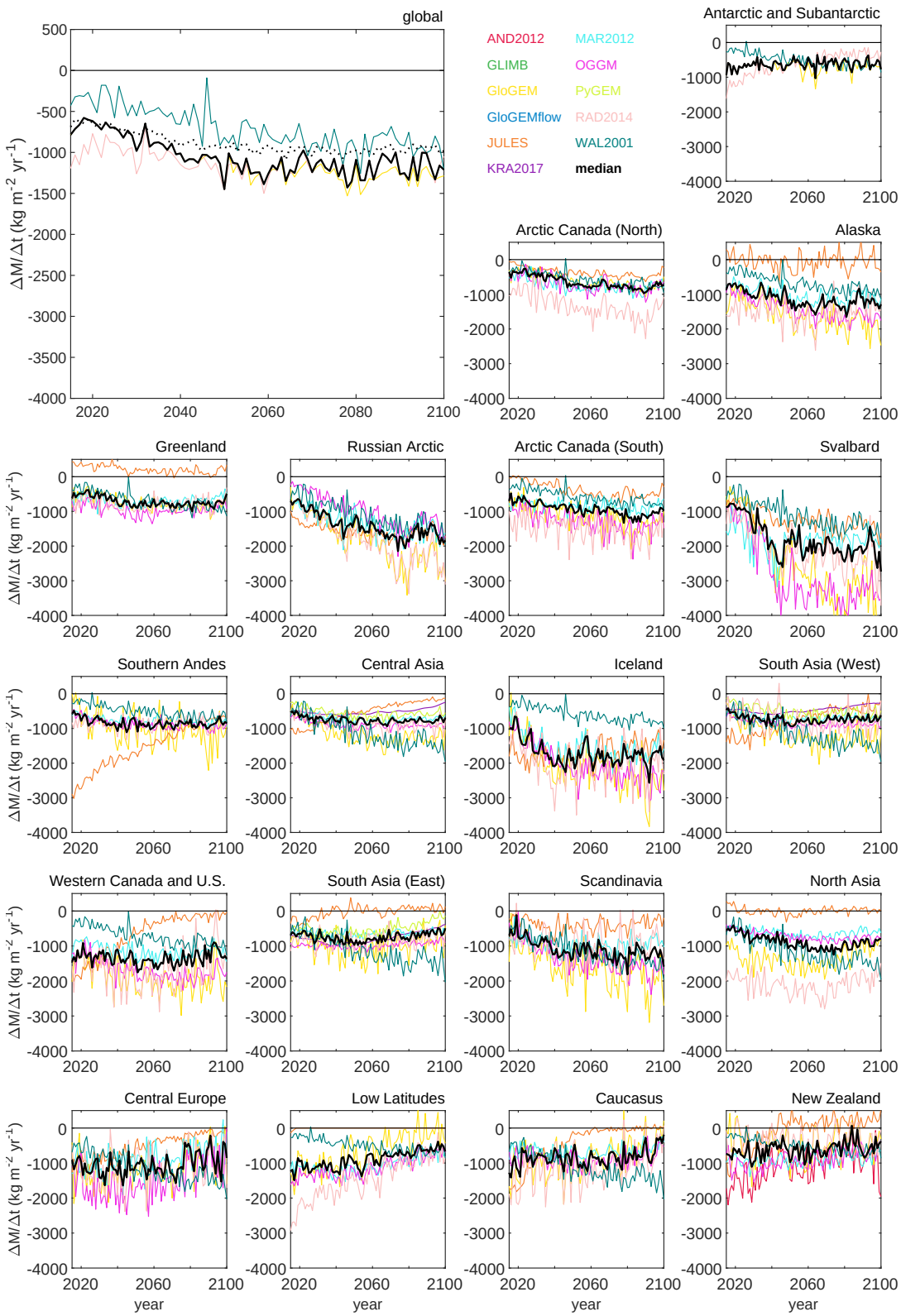

Figure S2 As Fig. S1, but for scenario RCP4.5.

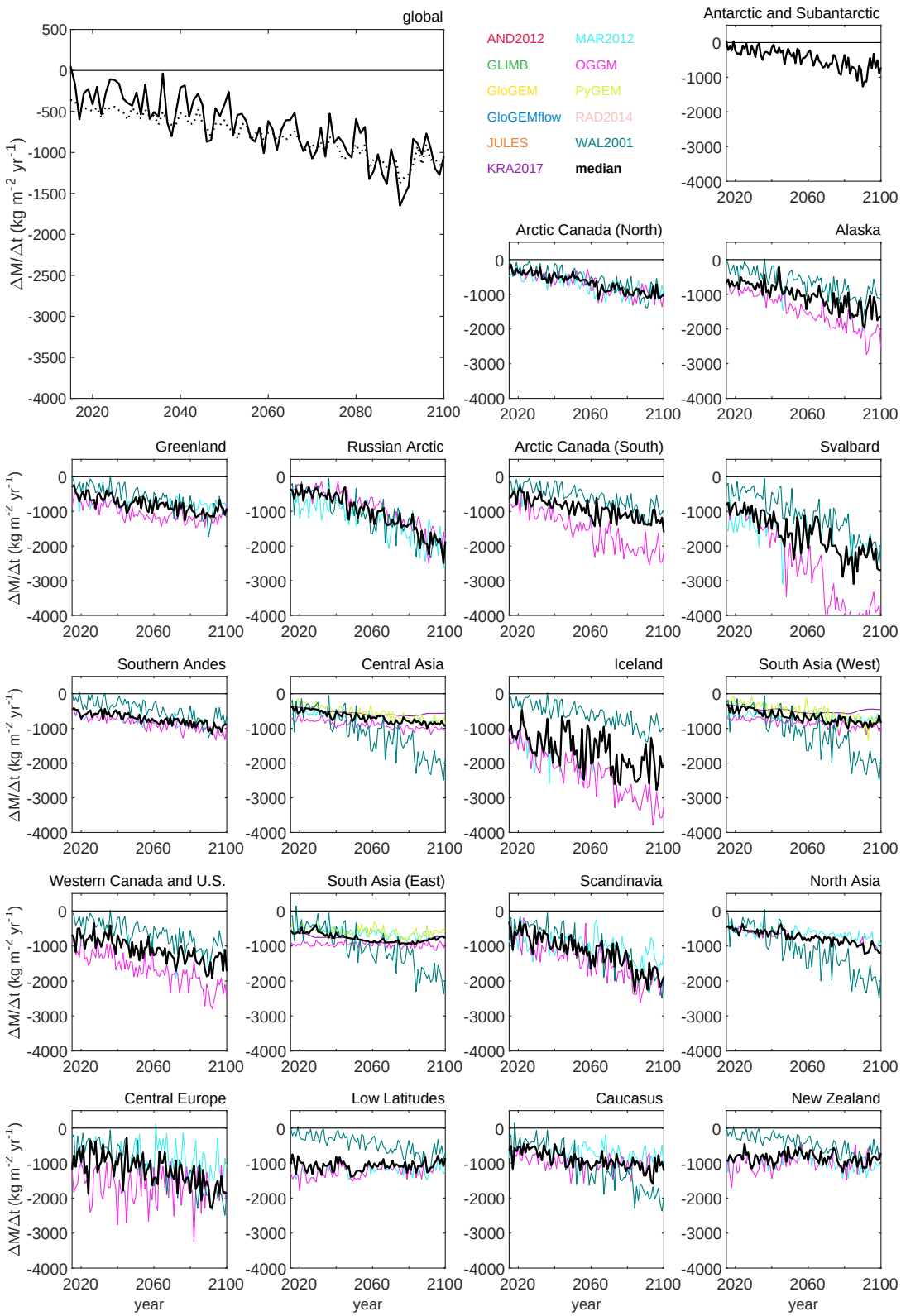

Figure S3 As Fig. S1, but for scenario RCP6.0.

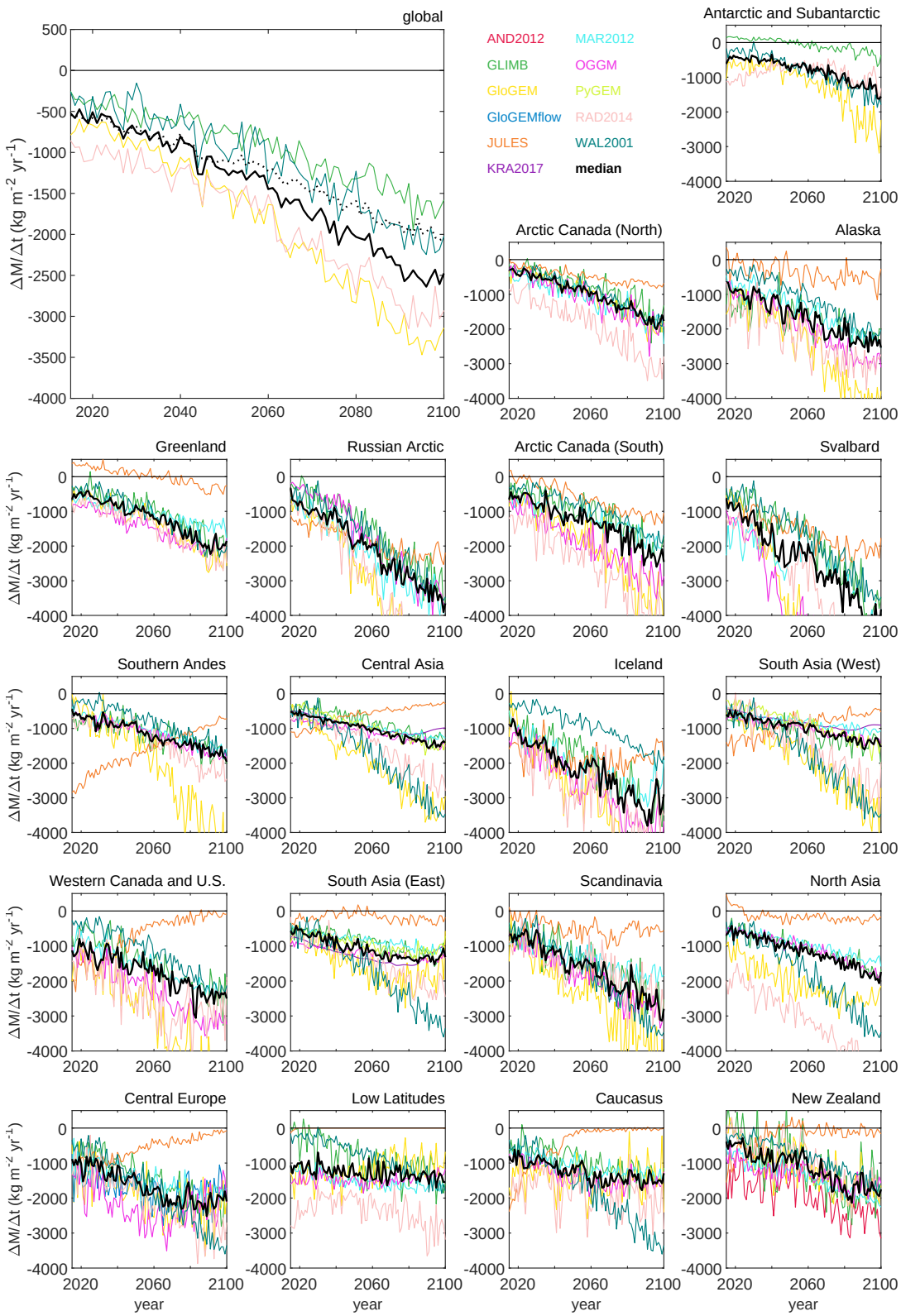

Figure S4 As Fig. S1, but for scenario RCP8.5.

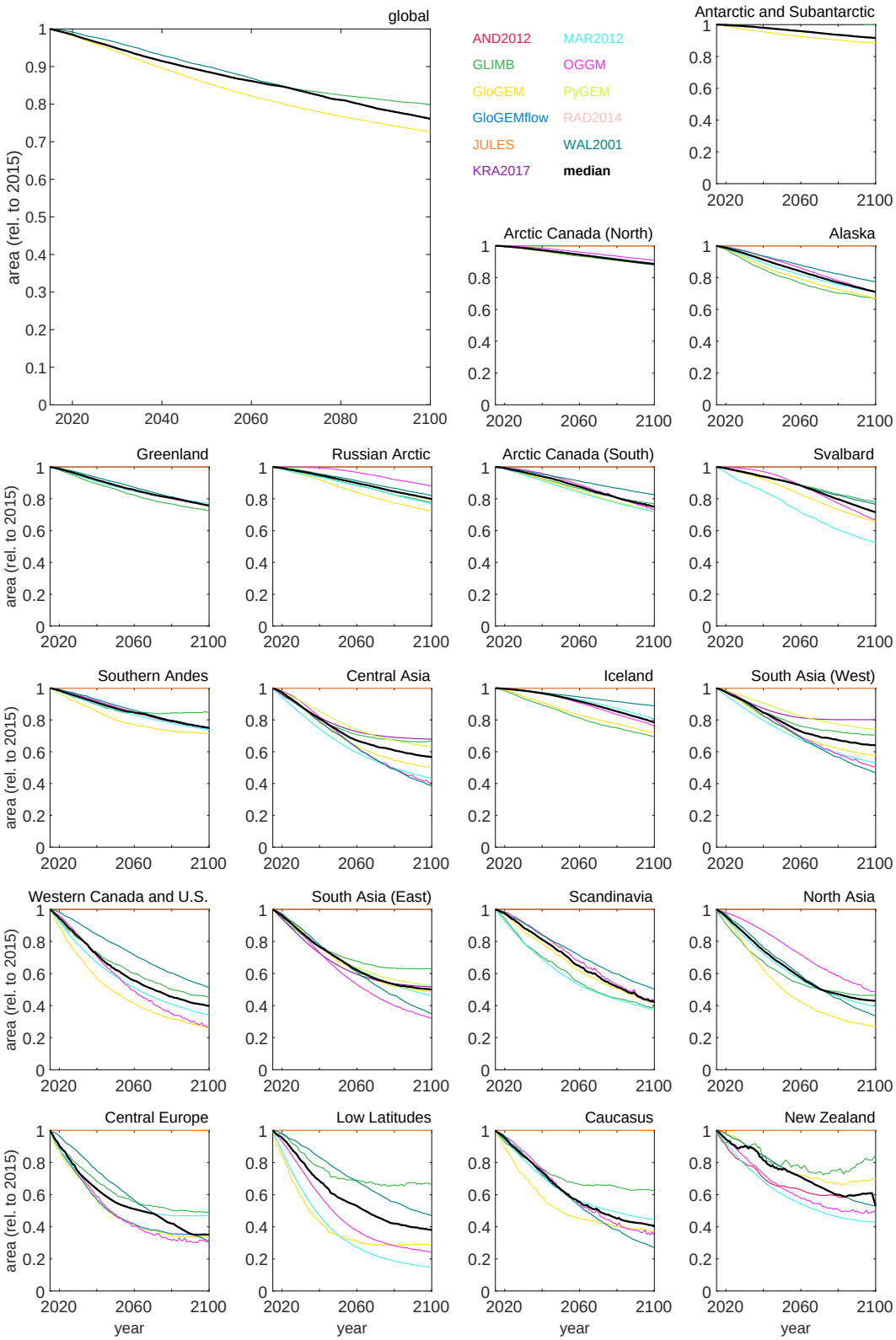

Figure S5 Glacier area change relative to 2015 as a function of time and glacier model, for scenario RCP2.6. Colored solid lines indicate the median of each glacier model's projections forced by different GCMs. Black lines indicate median of all glacier model medians covering that region.

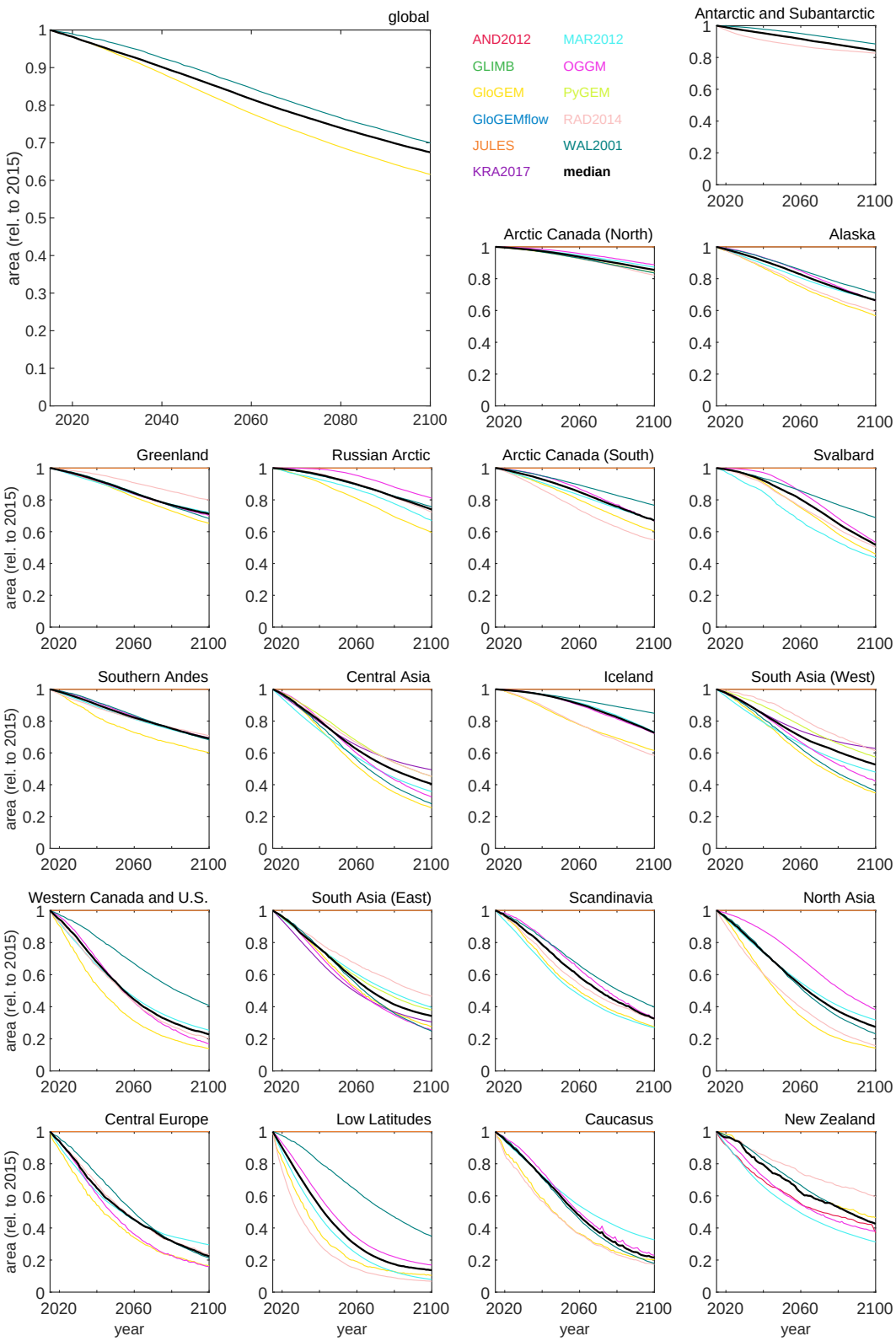

Figure S6 As Fig. S5, but for scenario RCP4.5.

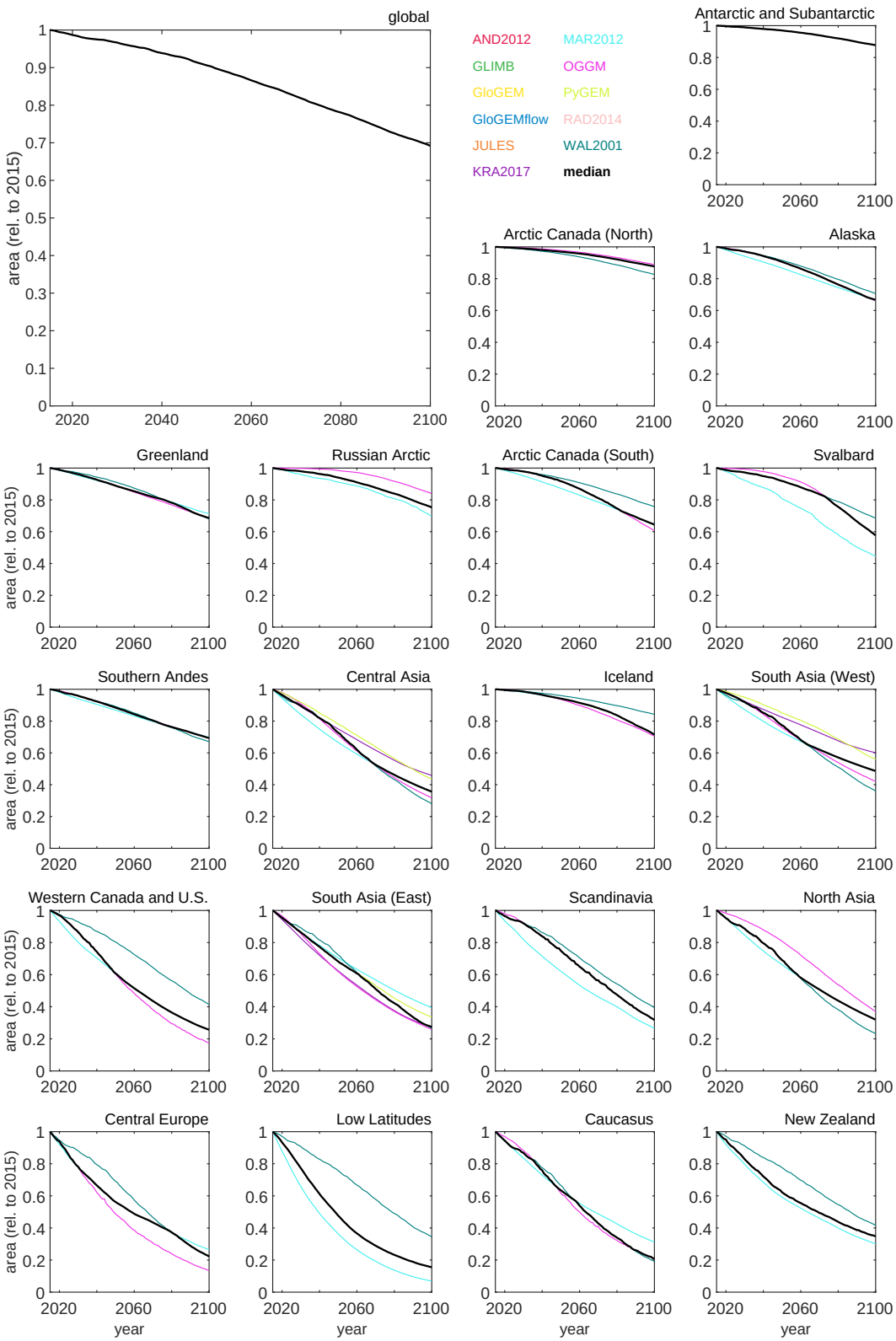

Figure S7 As Fig. S5, but for scenario RCP6.0.

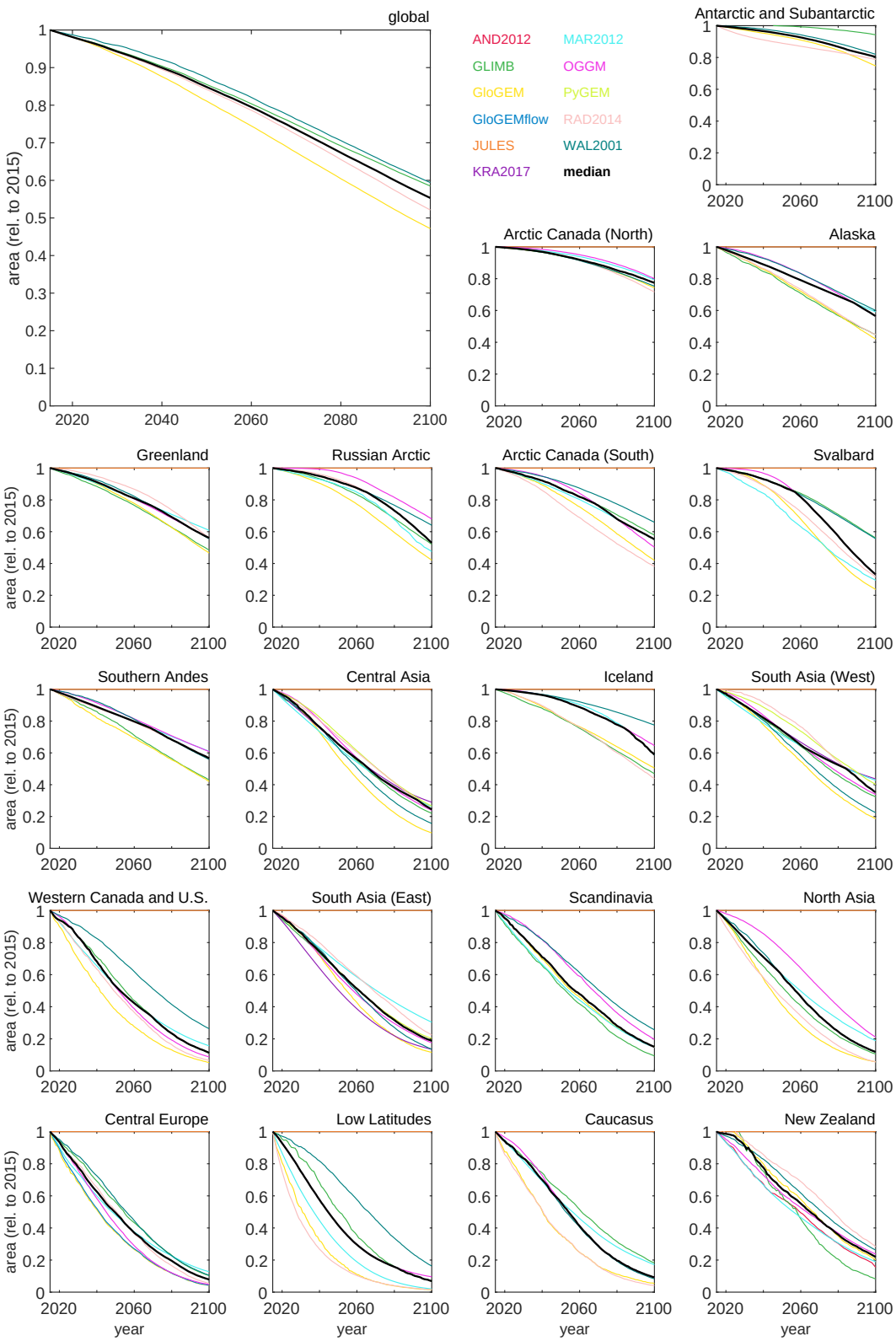

Figure S8 As Fig. S5, but for scenario RCP8.5.

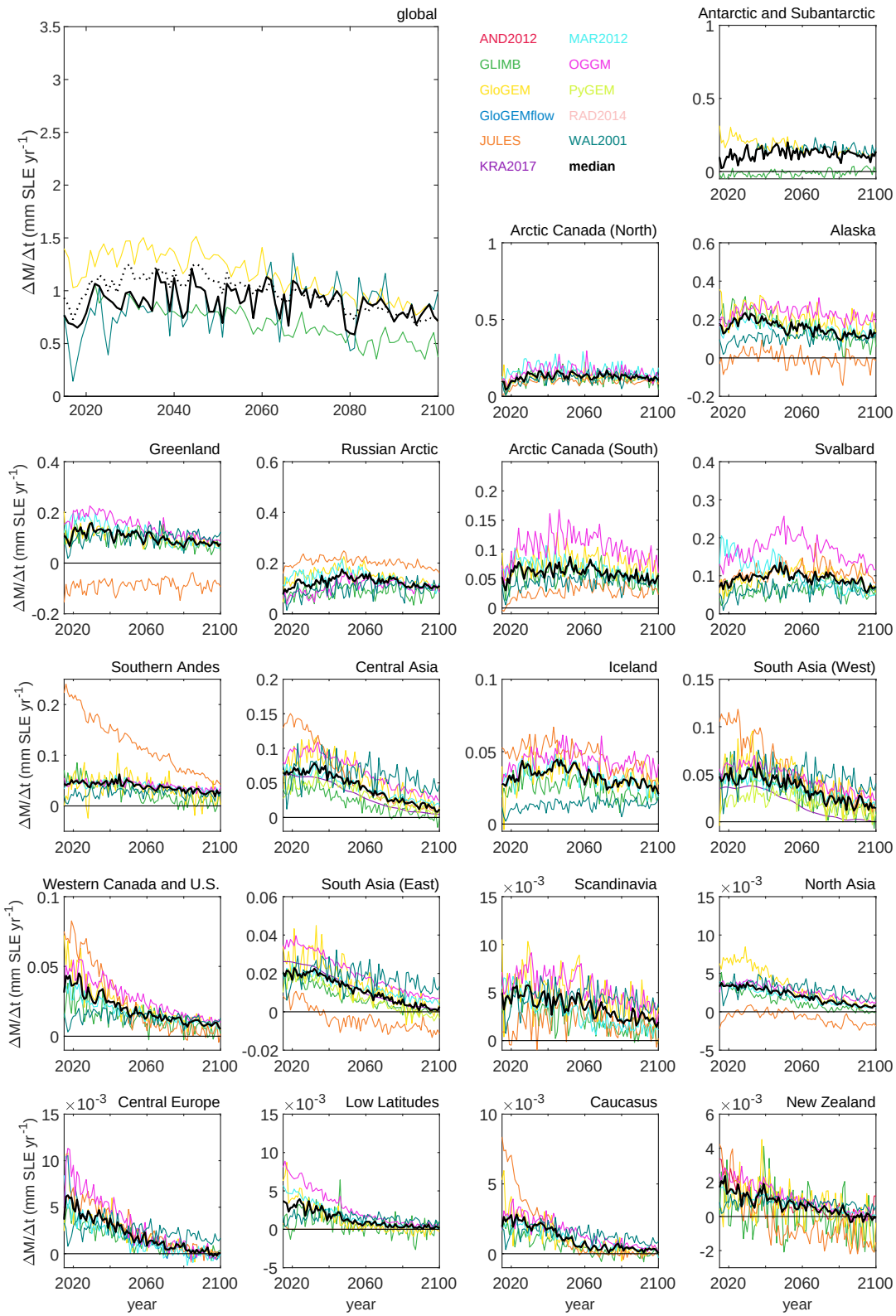

Figure S9 Rates of glacier mass loss in mm SLE yr^{-1} as a function of time and glacier model for scenario RCP2.6. Colored solid lines indicate median of each glacier model's projections forced by different GCMs. Global panel: dotted black line indicates sum of all regional ensemble medians. Solid black line indicates median of the medians of all glacier models with global coverage. Regional panels: black lines indicate median of all glacier model medians covering that region.

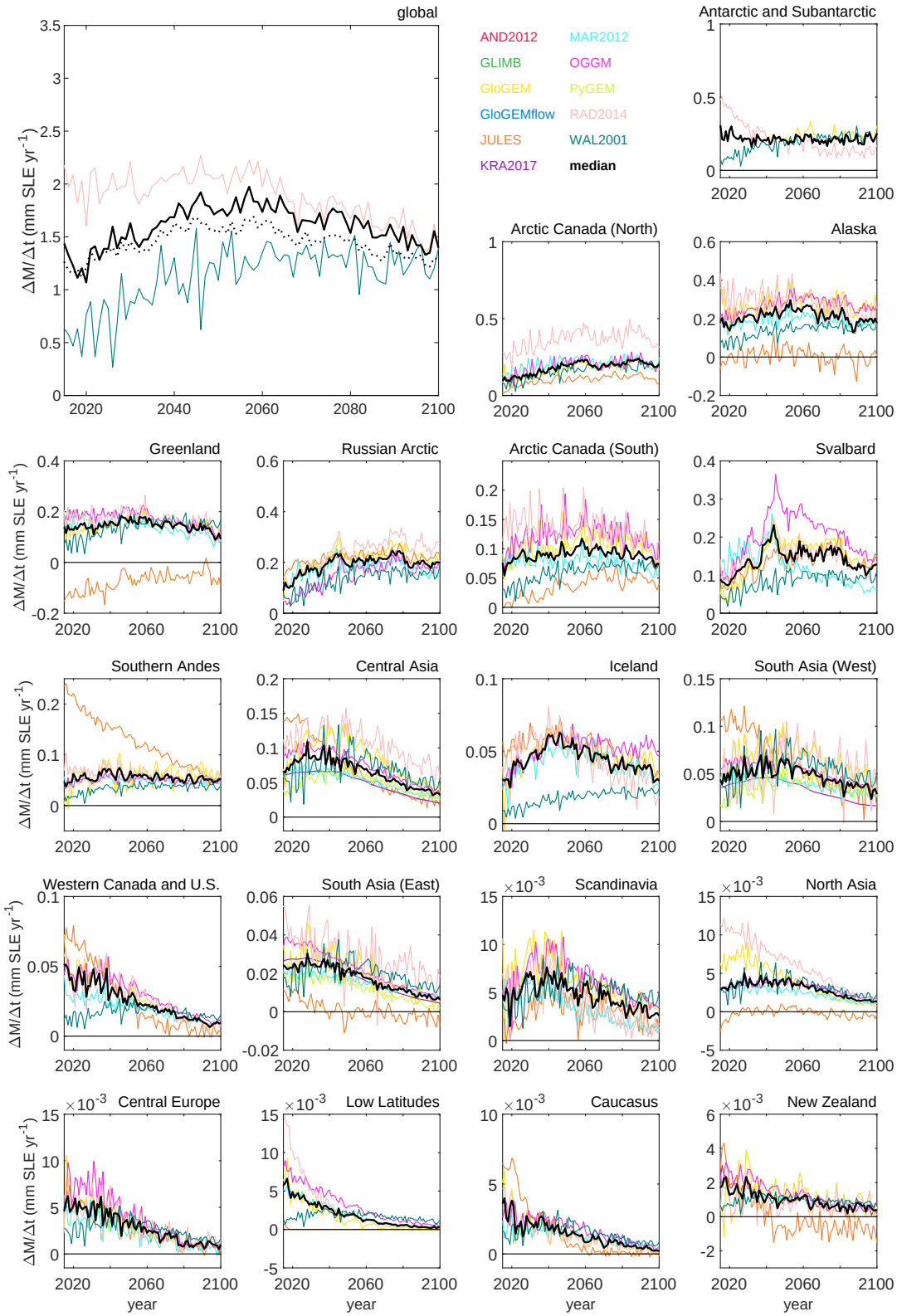

Figure S10 As Fig. S9, but for scenario RCP4.5.

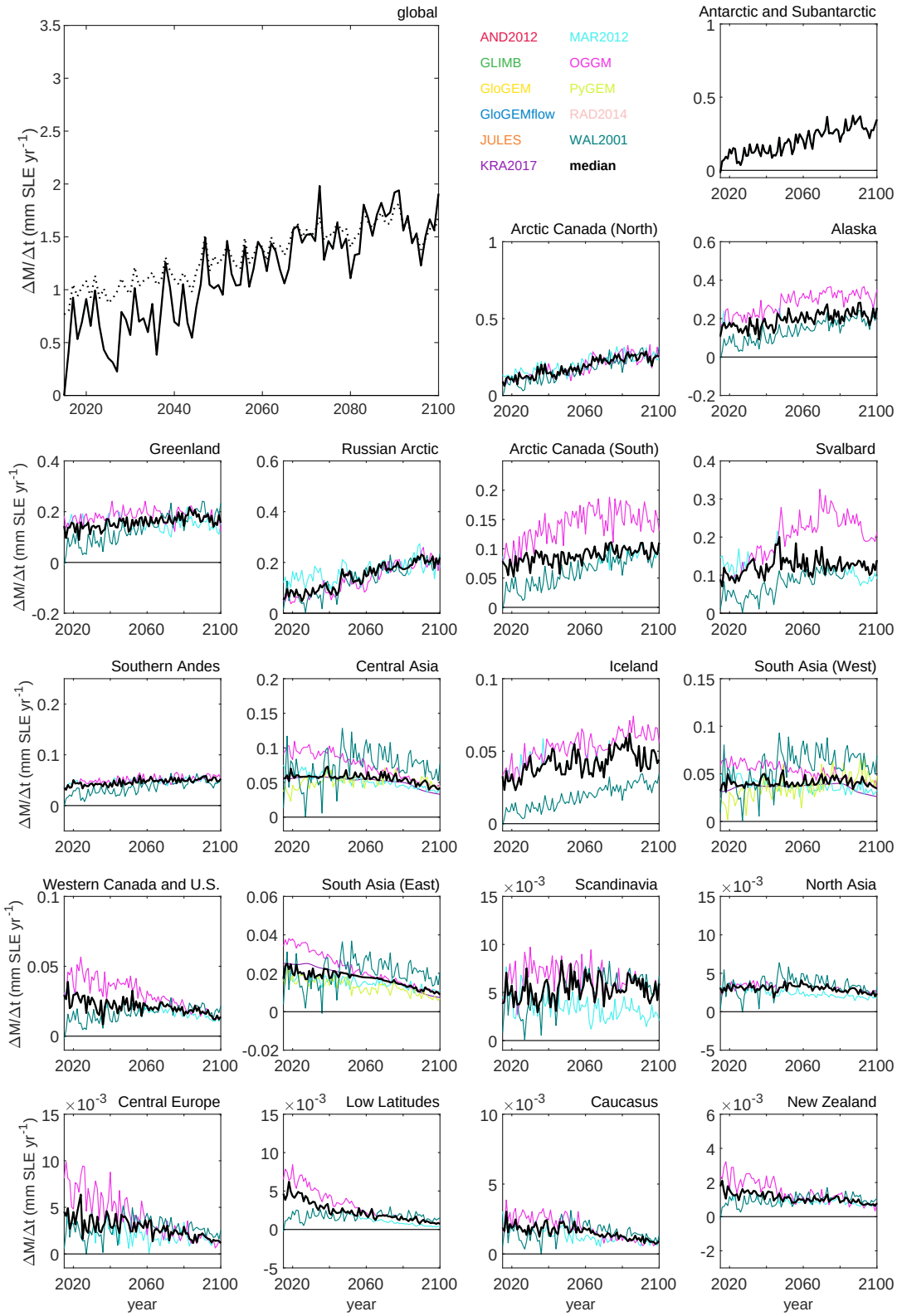

Figure S11 As Fig. S9, but for scenario RCP6.0.

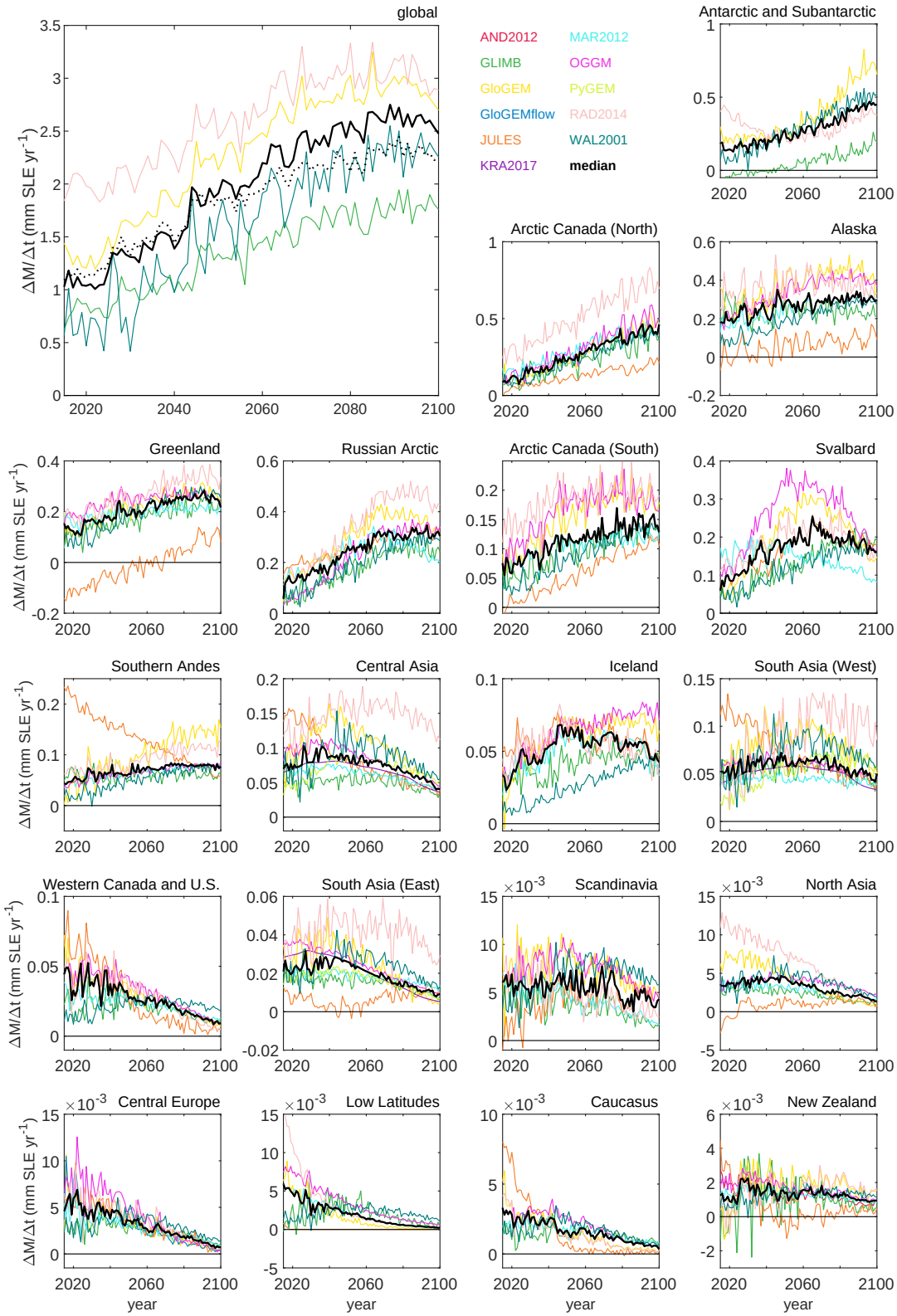

Figure S12 As Fig. S9, but for scenario RCP8.5.

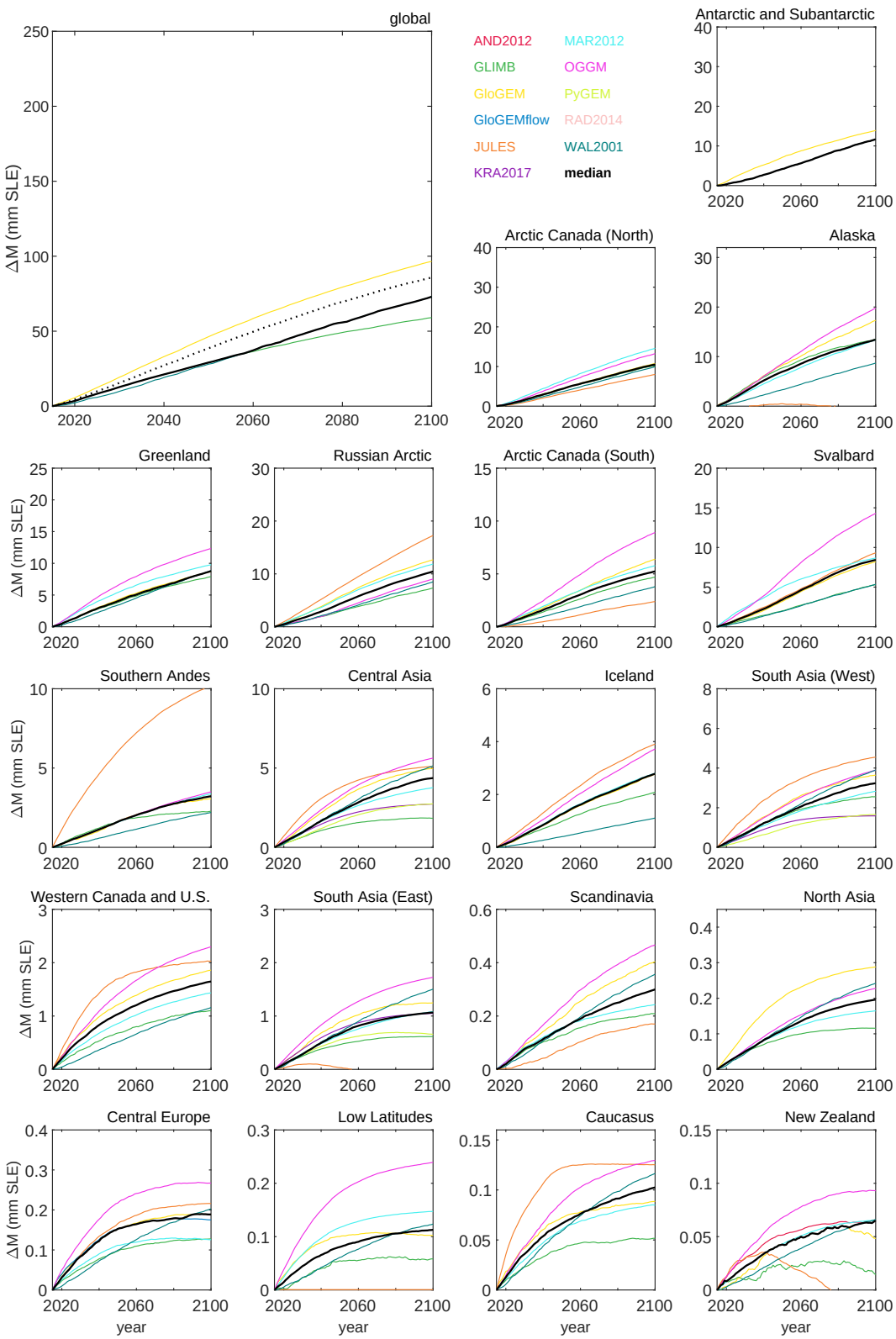

Figure S13 Temporally accumulated glacier mass loss in mm SLE since 2015 as a function of time and glacier model for scenario RCP2.6. Colored solid lines indicate median of each glacier model's projections forced by different GCMs. Global panel: dotted black line indicates sum of all regional ensemble medians. Solid black line indicates median of the medians of all glacier models with global coverage. Regional panels: black lines indicate median of all glacier model medians covering that region.

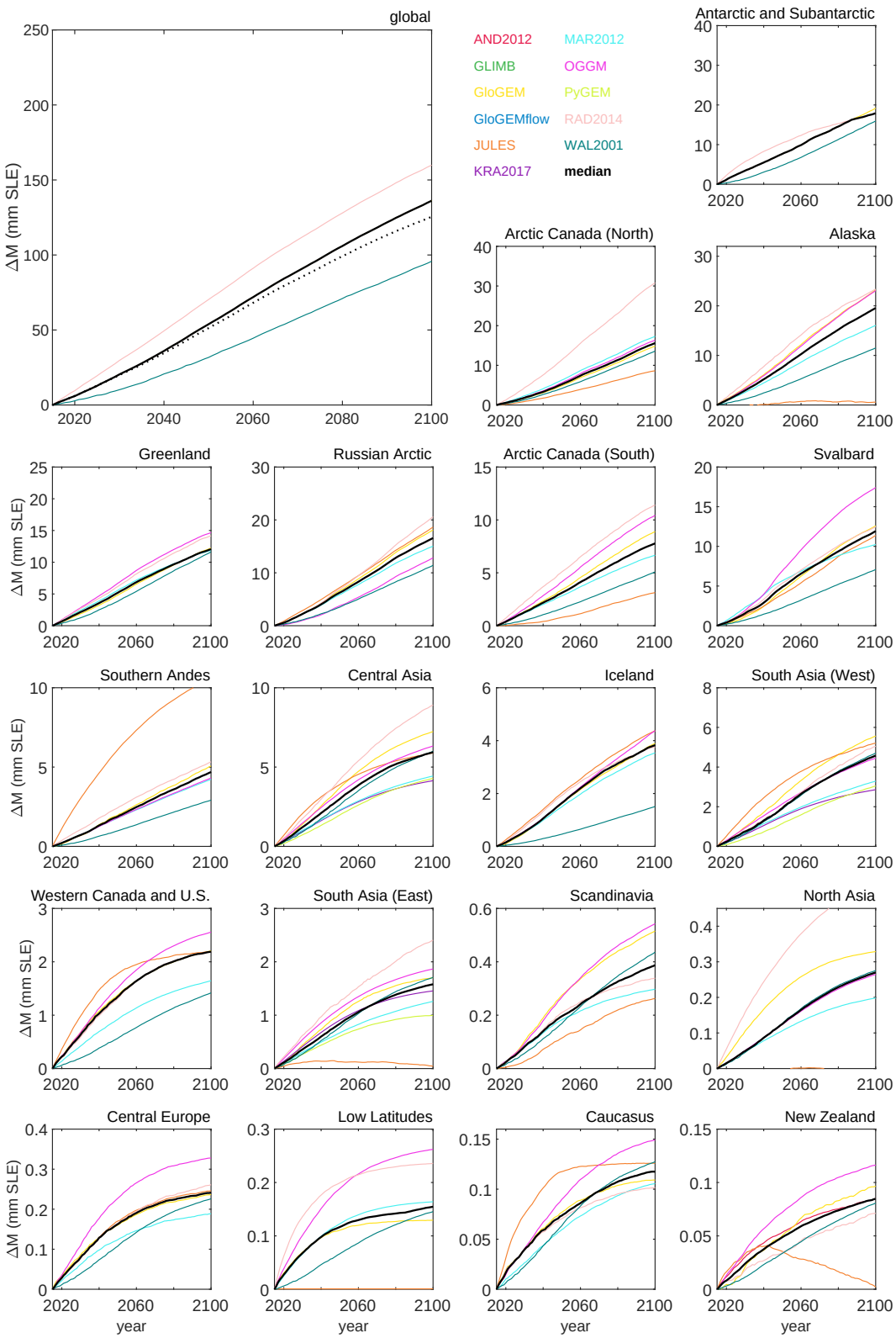

Figure S14 As Fig. S13 13, but for scenario RCP4.5.

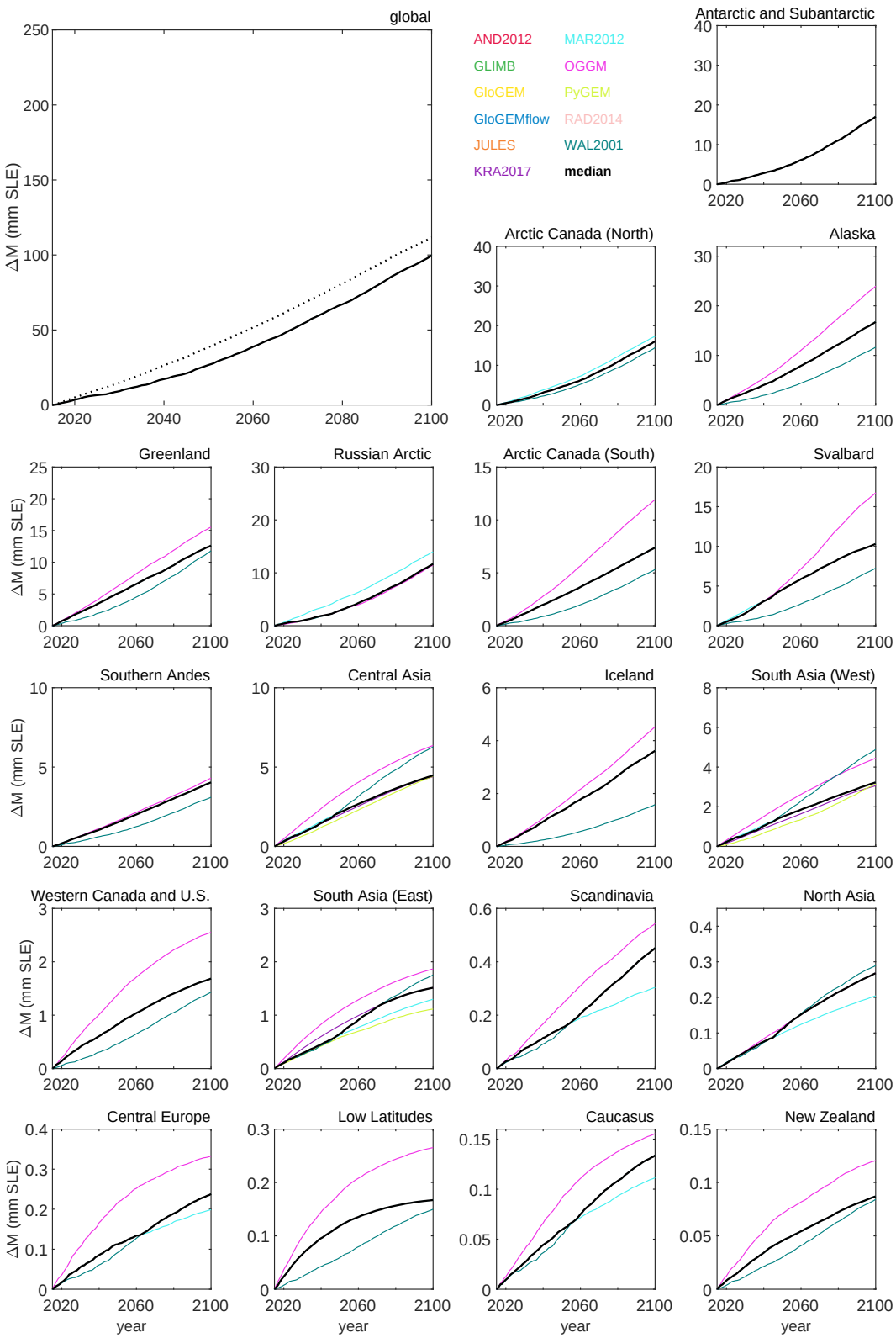

Figure S15 As Fig. S13 13, but for scenario RCP6.0.

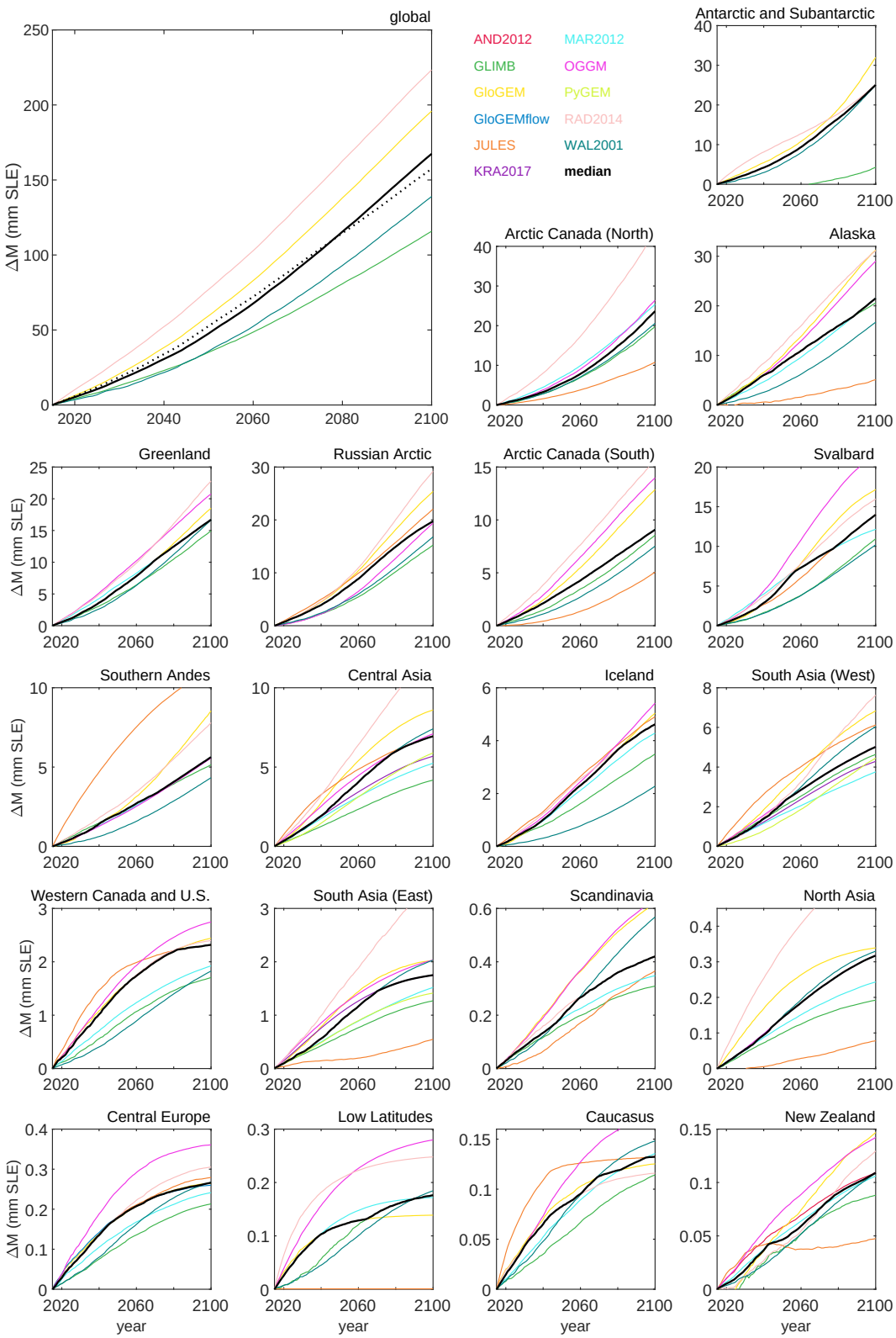

Figure S16 As Fig. S13 13, but for scenario RCP8.5.

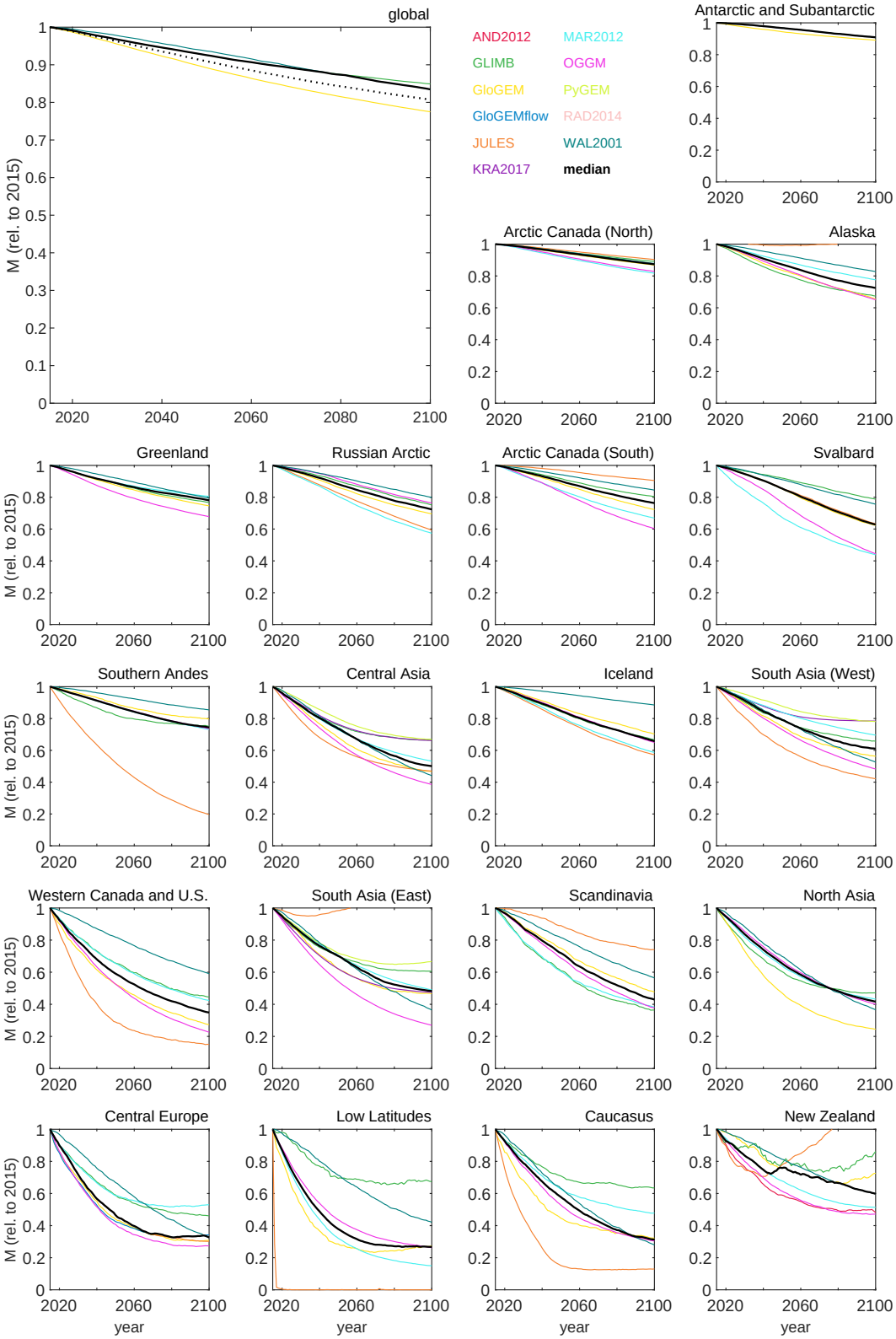

Figure S17 Glacier mass relative to 2015 as a function of time and glacier model for scenario RCP2.6. Colored solid lines indicate median of each glacier model's projections forced by different GCMs. Global panel: dotted black line indicates average of all regional ensemble medians, weighted by glacier mass of the respective region. Solid black line indicates median of the medians of all glacier models with global coverage. Regional panels: black lines indicate median of all glacier model medians covering that region.

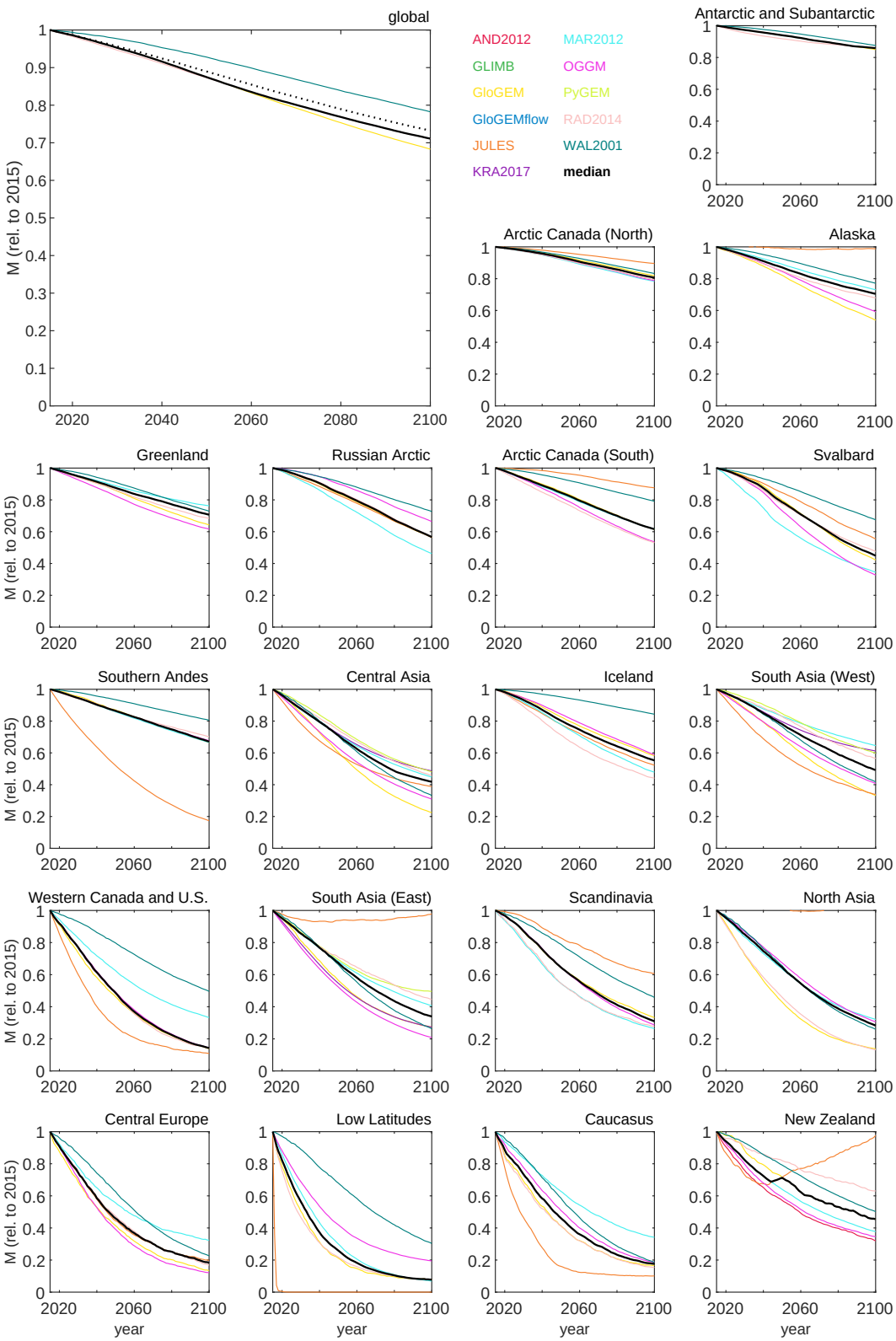

Figure S18 As Fig. S17, but for scenario RCP4.5.

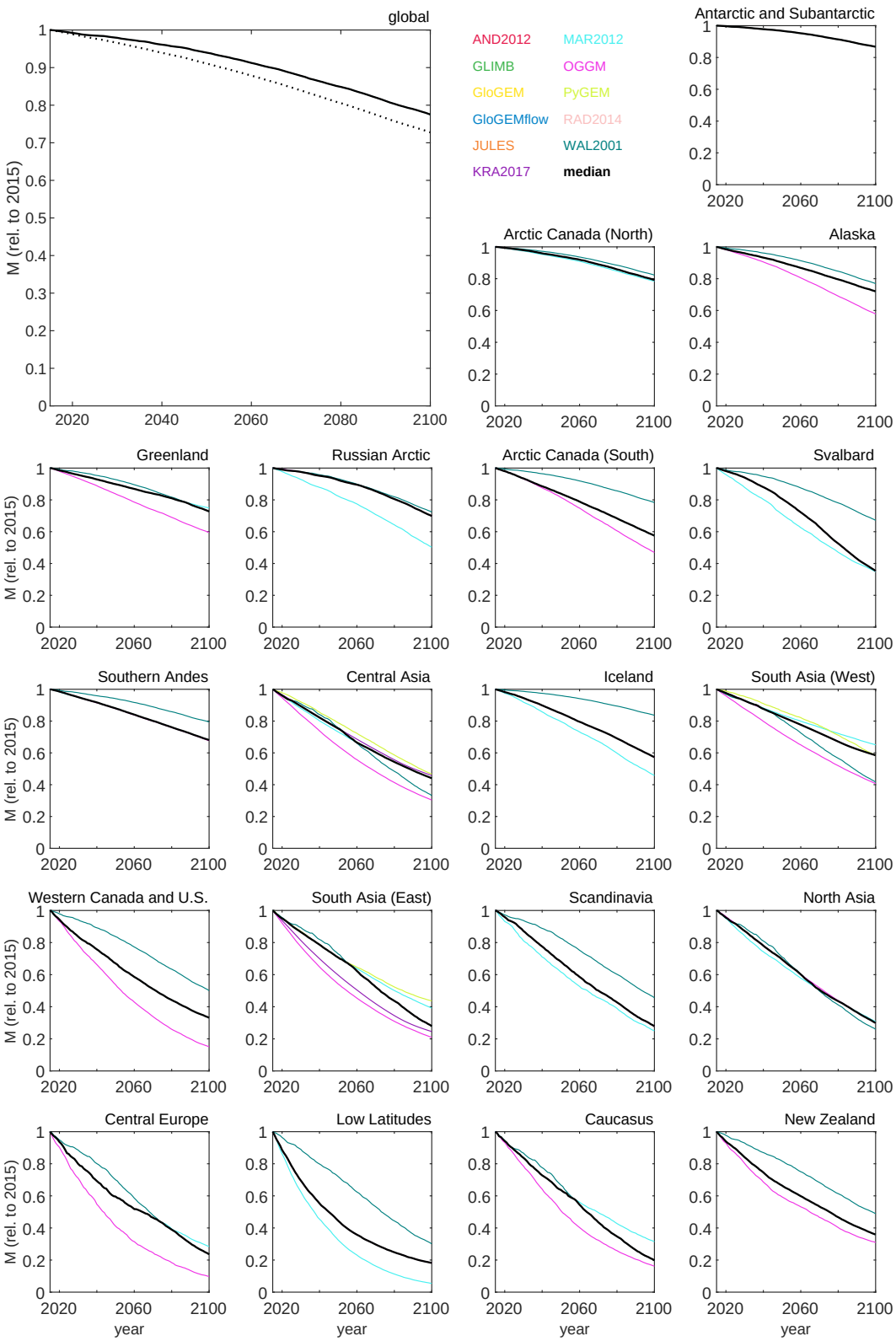

Figure S19 As Fig. S17, but for scenario RCP6.0.

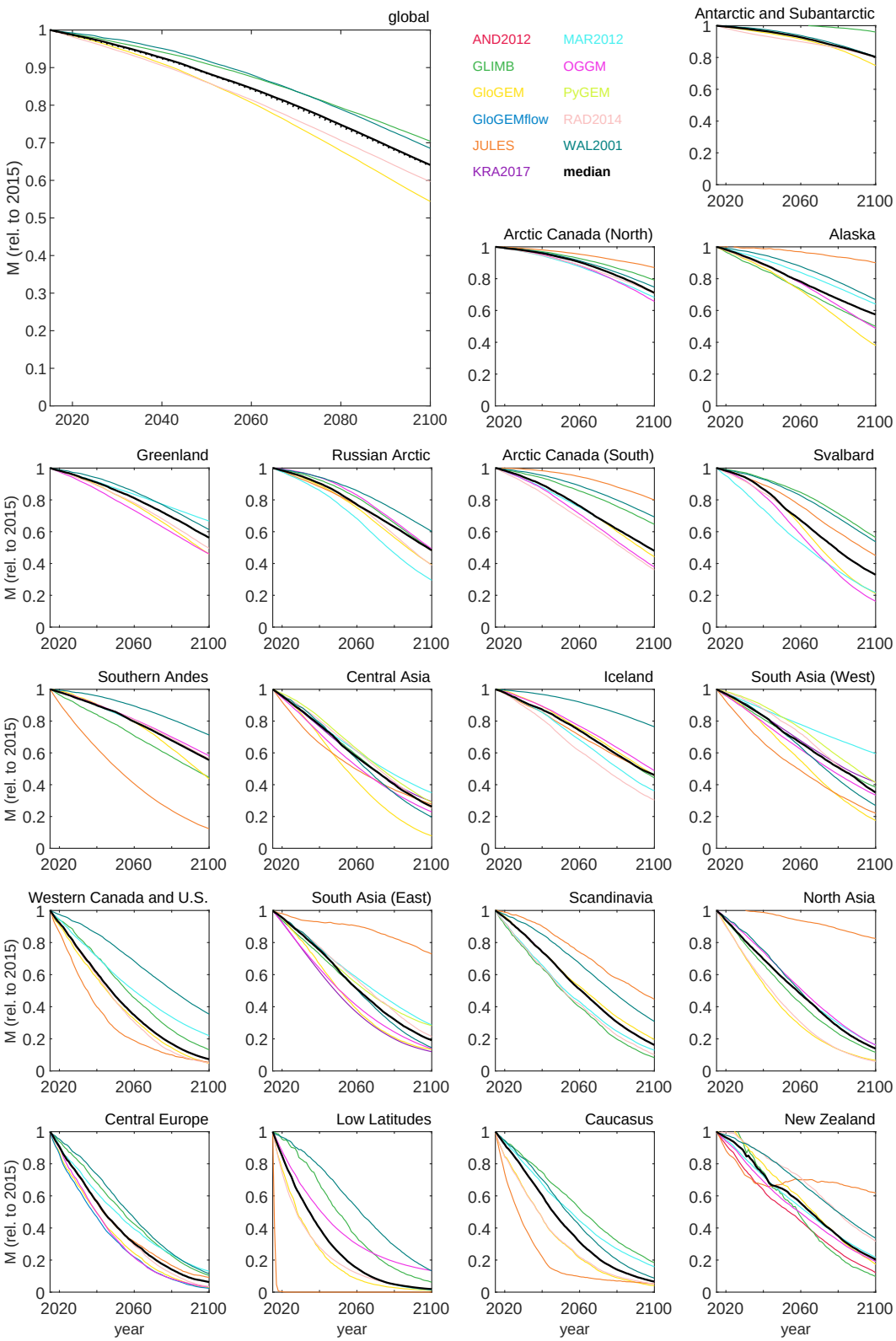

Figure S20 As Fig. S17, but for scenario RCP8.5.

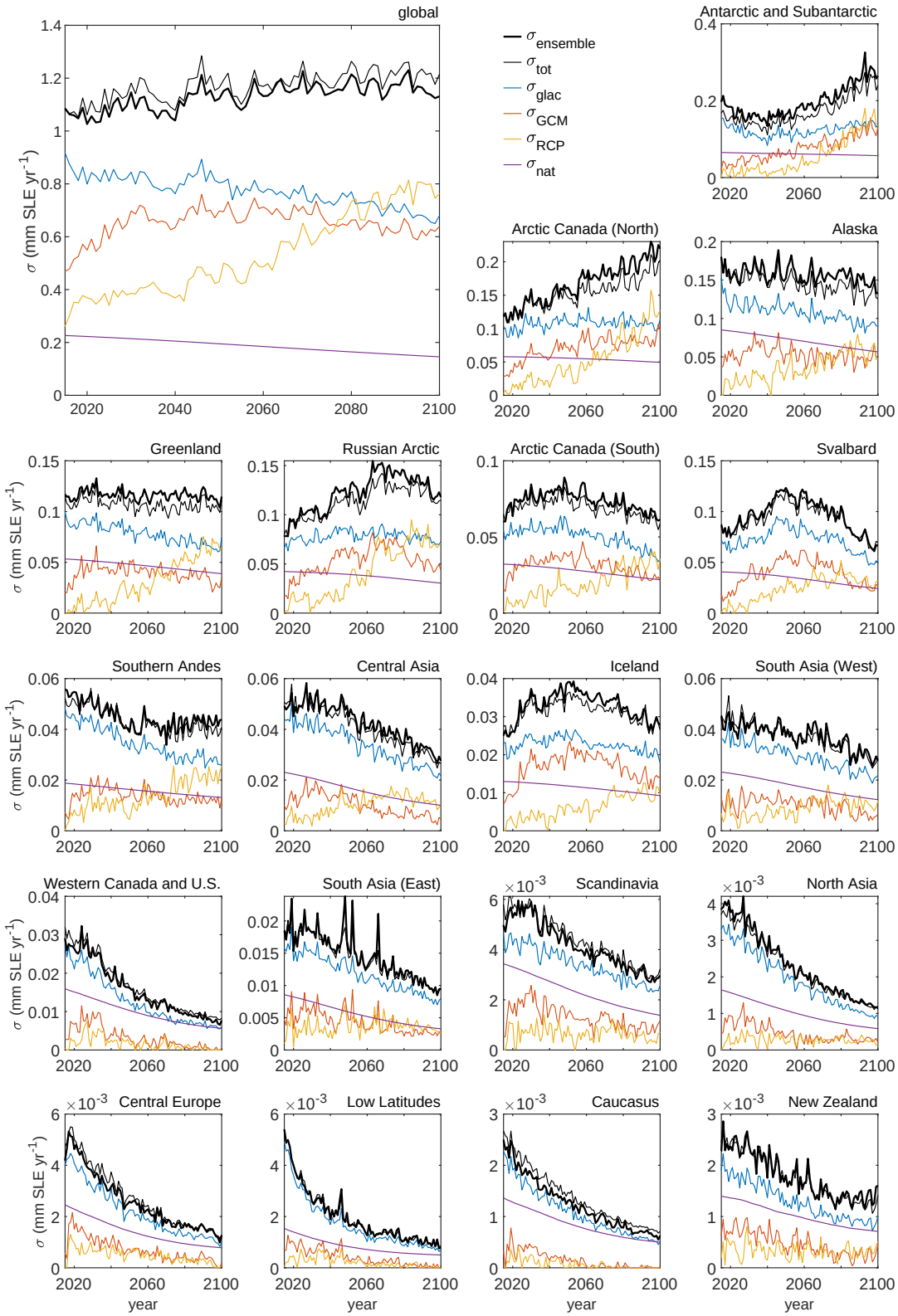

Figure S21 Contribution of each source of uncertainty (Equations 3-6) to the total uncertainty (σ_{tot}, Equation 2) of projected mass loss rates in mm SLE yr^{-1}. Also shown is the uncertainty obtained directly from the entire ensemble without any decomposition ($\sigma_{ensemble}$).

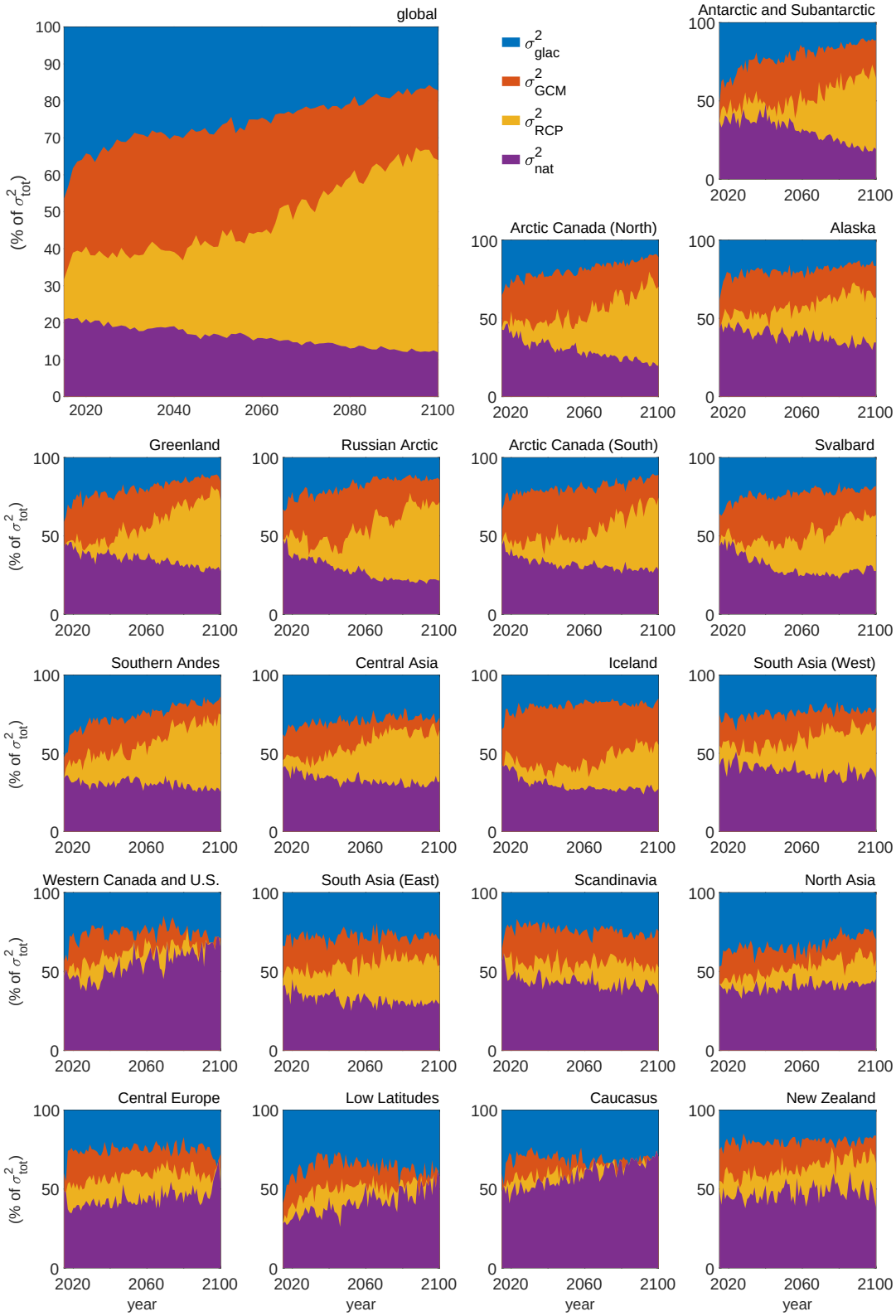

Figure S22 Relative contribution of each source of uncertainty to the total uncertainty (σ_{tot}, Equation 2) of projected mass loss rates in mm SLE yr^{-1}.

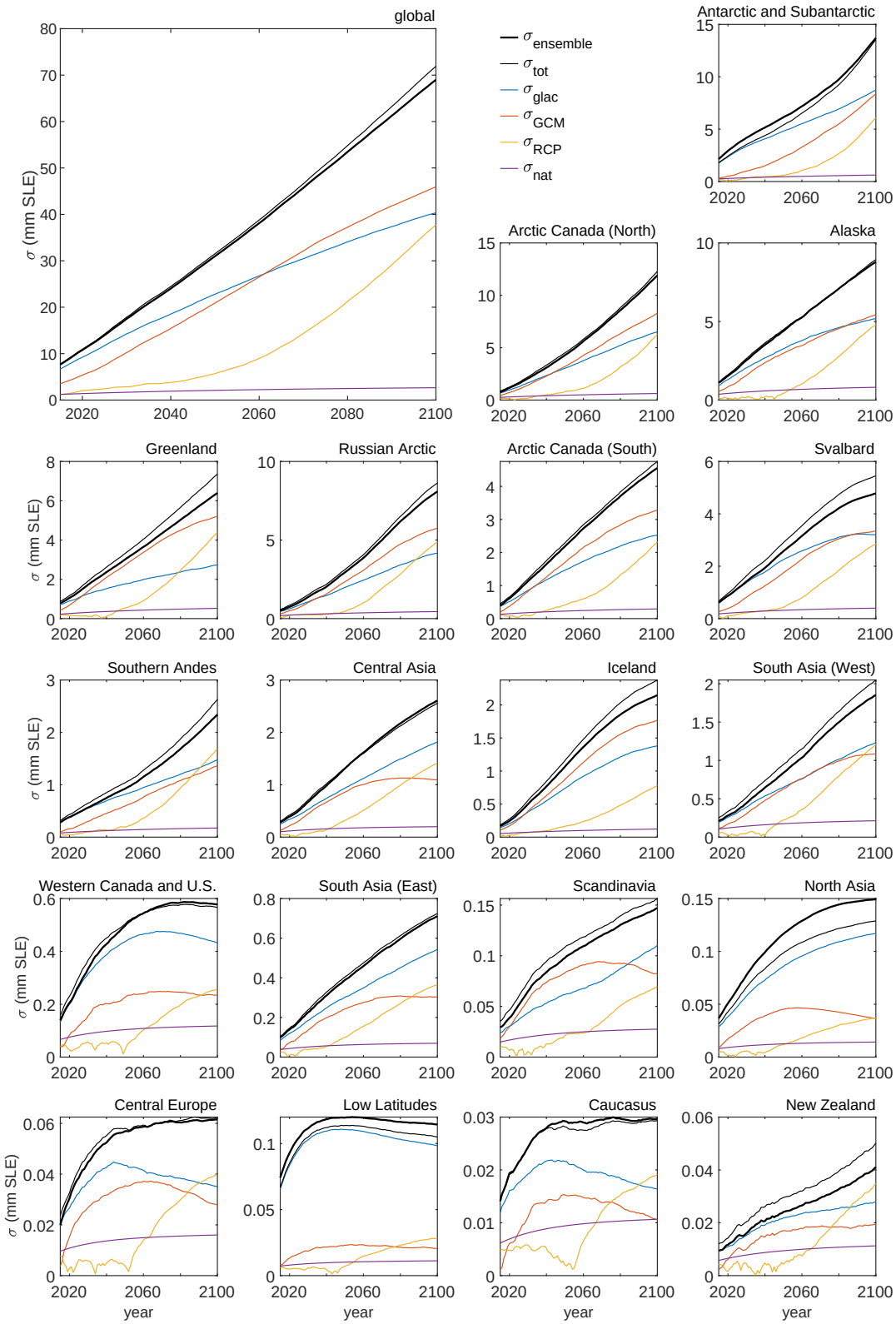

Figure S23 Contribution of each source of uncertainty (Equations 3-6) to the total uncertainty (σ_{tot}, Equation 2) of projected mass loss accumulated since 2015 in mm SLE. Also shown is the uncertainty obtained directly from the entire ensemble without any decomposition ($\sigma_{ensemble}$).

Table S1 Definition of years in each glacier model's submitted annual volume and area time series. Type of year indicates whether the mass changes were computed over calendar years or mass-balance years spanning roughly the period between two consecutive mass minima in the glaciers' annual cycle. Period refers to the specific period over which the annual mass changes were computed.[1]

Model	Type of year	Period (northern hemisph.)	Period (southern hemisph.)
AND2012	mass-balance	n/a	1 April - 31 March
GLIMB	mass-balance	1 Oct. - 30 Sept.	1 Oct. - 30 Sept.
GloGEM	mass-balance	1 Oct. - 30 Sept.	1 Apr. - 31 March
GloGEMflow	mass-balance	1 Oct. - 30 Sept.	n/a
JULES	calendar	1 Jan. - 31 Dec.	1 Jan. - 31 Dec.
KRA2017	calendar	1 Jan. - 31 Dec.	n/a
MAR2012	mass-balance	1 Oct. - 30 Sept.	1 Apr. - 31 March
OGGM	mass-balance	1 Oct. - 30 Sept.	1 Apr. - 31 March
PyGEM	mass-balance	1 Oct. - 30 Sept.	n/a
RAD2014	mass-balance	1 Sept. - 31 Aug. (> 75°N); 1 Oct. - 30 Sept. (< 75°N)	1 March. - 28 Feb. (< –75°S); 1 Apr. - 31 March (> 75°S)
WAL2001	calendar	1 Jan. - 31 Dec.	1 Jan. - 31 Dec.

[1] Each modeling group submitted the time series of annual glacier volume and area for the years 2015 - 2100 (referring to the beginning of the year). However, the definition of a year differed between the different glacier models. The submitted data from eight groups referred to mass-balance years, while the data from the other three groups referred to calendar years. In addition, the definition of a mass-balance year differed between the models. The discrepancy between calendar and mass-balance years was not corrected for. However, in Equation 1, for each model and region, ΔT was computed over the time period that corresponds to the model's and region's definition of a year based on monthly data.

Table S2 Summary of bias correction (removing differences between GCM climatology and observed climatology), downscaling (accounting for the differences of the scales of GCM resolution and mountain topography), as well as calibration and evaluation/validation procedures of modeled mass balance for each glacier model. Bias corrections are typically derived from comparison to observation-based gridded data sets, while further adjustments as part of downscaling are often derived from literature-based or calibrated model parameters. In some models, bias correction and downscaling are lumped into one step. We do not include information in this table concerning the models' treatment of variability of atmospheric conditions within the domain of an individual glacier.

	AND2012	GLIMB	GloGEM	GloGEMflow	JULES	KRA2017
bias correction	additive temperature bias correction and multiplicative precipitation bias correction, applied monthly based on local temperature and precipitation interpolated from station data (at 0.05° resolution)	additive temperature bias correction and multiplicative seasonal temperature amplitude correction based on ERA-Interim; see "downscaling" for precipitation treatment	additive temperature bias correction and multiplicative precipitation bias correction; adjustment of interannual variability for both, based on ERA-Interim	additive temperature bias correction and multiplicative precipitation bias correction; adjustment of interannual variability for both, based on ERA-Interim	additive temperature bias correction and multiplicative bias correction for precipitation, surface pressure, long and shortwave radiation and wind speed using WFDEI climatology (Weedon et al.; 2014)	additive temperature and precipitation bias correction based on WFDEI climatology (Weedon et al.; 2014)
downscaling	constant temperature lapse rate; precipitation correction factor	constant precipitation correction factor	spatially and seasonally varying temperature lapse rate; precipitation correction factor	spatially and seasonally varying temperature lapse rate; precipitation correction factor	constant temperature lapse rate, constant scaling factor for wind speed; see "bias correction" for adjustment of other variables	constant temperature lapse rate; no further adjustment of precipitation
calibration	individual glaciers are calibrated to regional specific mass change 1976-2016 (-0.3 m w.e. a^{-1}) from unpublished data	regional calibration to regional mean specific mass change 2003-2009 from Gardner et al. (2013)	individual glaciers are calibrated to regional specific mass change 2003-2009 from Gardner et al. (2013); frontal ablation calibrated to match regional sum from various studies	for individual glaciers, using glacier specific mass change from WGMS (2017), or relying on estimates from nearby and similarly-size glaciers	regional calibration using elevation-dependent annual specific mass change from WGMS (2017)	optimization of mass balance gradient using observed regional mass balances from various studies
evaluation/validation	for individual glaciers using direct annual mass balance observations from WGMS (2017)	for individual glaciers using direct annual mass balance observations from WGMS (2017)	for individual glaciers using direct seasonal mass balance observations (glacier-wide, elevation bands, point balance) from WGMS (2017)	for individual glaciers using direct annual mass balance observations from WGMS (2017)	regional evaluation using elevation-dependent winter and summer specific mass balance observations from WGMS (2017)	regional evaluation using independent remotely-sensed length change, ELA and snowline data from Gardelle et al. (2013) and Scherler et al. (2011)

Table S2 continued

	MAR2012	OGGM	PyGEM	RAD2014	WAL2001
bias correction	additive temperature and precipitation bias correction based on CRU CL2.0 climatology	additive temperature and precipitation bias correction based on CRU CL2.0 climatology; interannual temperature variability scaled to CRU TS	additive temperature bias correction and multiplicative precipitation bias correction, adjustment of interannual variability for both, based on ERA-Interim	additive temperature bias correction using ERA-40, multiplicative precipitation bias correction based on Beck et al. (2005); adjustment of interannual variability for both	no bias correction, model uses only temperature and precipitation anomalies
downscaling	spatially varying temperature lapse rate; precipitation correction factor	constant temperature lapse rate and precipitation correction factor	spatially and temporally varying temperature lapse rate; no further adjustment of precipitation	spatially varying temperature lapse rate and precipitation correction factor	none
calibration	for individual glaciers, using direct mass balance observations from WGMS (2017)	for individual glaciers, using direct mass balance observations from WGMS (2017)	for individual glaciers, using geodetic mass balance observations from Shean et al. (2020)	for individual glaciers, using seasonal mass balance profiles from 36 glaciers from WGMS (2017), for regions using regionally compiled glaciological and geodetic mass change from Cogley (2009)	for 12 individual glaciers, using mass change observations from Zuo and Oerlemans (1997)
evaluation/validation	for individual glaciers, using glaciological mass balance observations from WGMS (2017), leave-one-glacier-out cross-validation	for individual glaciers, using glaciological mass balance observations from WGMS (2017), leave-one-glacier-out cross-validation	for individual glaciers, using geodetic and glaciological measurements from WGMS (2017) and equilibrium line altitudes from Gardelle et al. (2013)	for individual glaciers, using seasonal mass change measurements from Dyurgerov (2010)	parameter sensitivity analysis, details in Slangen and van de Wal (2011)

References

Beck, C., Grieser, J. and Rudolf, B. (2005). A new monthly precipitation climatology for the global land areas for the period 1951 to 2000, *Climate Status Report 2004*, German Weather Service, Offenbach, Germany, pp. 181–190.

Cogley, J. G. (2009). Geodetic and direct mass-balance measurements: comparison and joint analysis, *Annals of Glaciology* **50**(50): 96–100.

Dyurgerov, M. (2010). Reanalysis of glacier changes: from the IGY to the IPY, 1960–2008, *Data of Glaciological Studies* **108**: 1–116.

Gardelle, J., Berthier, E., Arnaud, Y. and Kääb, A. (2013). Region-wide glacier mass balances over the Pamir-Karakoram-Himalaya during 1999–2011, *The Cryosphere* **7**(4): 1263–1286.

Gardner, A. S., Moholdt, G., Cogley, J. G., Wouters, B., Arendt, A. A., Wahr, J., Berthier, E., Hock, R., Pfeffer, W. T., Kaser, G., Ligtenberg, S. R. M., Bolch, T., Sharp, M. J., Hagen, J. O., van den Broeke, M. R. and Paul, F. (2013). A reconciled estimate of glacier contributions to sea level rise: 2003 to 2009, *Science* **340**: 852–857.

Scherler, D., Bookhagen, B. and Strecker, M. R. (2011). Spatially variable response of himalayan glaciers to climate change affected by debris cover, *Nature Geoscience* **4**(3): 156–159.

Shean, D. E., Bhushan, S., Montesano, P., Rounce, D. R., Arendt, A. and Osmanoglu, B. (2020). A systematic, regional assessment of high mountain asia glacier mass balance, *Frontiers in Earth Science* **7**: 363.

Slangen, A. B. A. and van de Wal, R. S. W. (2011). An assessment of uncertainties in using volume-area modelling for computing the twenty-first century glacier contribution to sea-level change, *The Cryosphere* **5**(3): 673–686.

Weedon, G. P., Balsamo, G., Bellouin, N., Gomes, S., Best, M. J. and Viterbo, P. (2014). The WFDEI meteorological forcing data set: WATCH forcing data methodology applied to ERA-interim reanalysis data, *Water Resources Research* **50**: 7505–7514.

WGMS (2017). Fluctuations of glaciers database.

Zuo, Z. and Oerlemans, J. (1997). Contribution of glacier melt to sea-level rise since AD 1865: a regionally differentiated calculation, *Climate Dynamics* **13**: 835–845.